the glue density is at the origin of the claim that measuring the yield of strangeness probes the presence and abundance of glue, which is a specific property of QGP.

In the model calculations presented, the fireball begins to expand in the transverse direction instantly at the full velocity. For this reason, the initial drop in temperature is very rapid. This defect also makes the transverse size at the end of the expansion too large, $R_\perp \simeq R_0 + t_f/\sqrt{3} \simeq 9$ fm, compared with the results of HBT analysis, Fig. 9.11. This can easily be fixed by introducing a more refined model of the transverse velocity, which needs time to build up. The yield of strangeness may slightly increase in such a refinement, since the fireball will spend more time near to the high initial temperature.

The RHIC results presented are typical for all collision systems. In the top SPS energy range, the initial temperature reached is certainly less (by 10%–20%) than that in the RHIC 130-GeV run, and the baryon number in the fireball is considerably greater; however, the latter difference matters little for production of strangeness, which is driven by gluons. A model similar to the above yields $\gamma_{\rm s}^{\rm QGP} \simeq 0.6$–$0.7$, the upper index reminds us that in this section the strangeness occupancy factor $\gamma_{\rm s}$ refers to the property of the deconfined phase. The experimental observable directly related to $\gamma_{\rm s}^{\rm QGP}$ is the total yield of strangeness per participating baryon. We will return to discuss the significance of these results in section 19.4.

18 The strangeness background

18.1 The suppression of strange hadrons

Since the matter around us does not contain valence strange quarks, all strange hadrons produced must contain newly made strange and antistrange quarks. If strangeness is to be used as a diagnostic tool for investigating QGP, we need to understand this background rate of production of strange hadrons. In that context, we are interested in measuring how often, compared with pairs of light quarks, strange quarks are made. One defines for this purpose the strangeness-suppression factor[†]

$$W_{\rm s} = \frac{2\langle {\rm s}\bar{\rm s}\rangle}{\langle {\rm u}\bar{\rm u}\rangle + \langle {\rm d}\bar{\rm d}\rangle}. \tag{18.1}$$

In $W_{\rm s}$, all newly made $\rm s\bar{s}$, $\rm u\bar{u}$, and $\rm d\bar{d}$ quark pairs are counted.

If strangeness were to be as easily produced as light u and d quarks, we would find $W_{\rm s} \to 1$. To obtain the experimental value for $W_{\rm s}$, a careful study of produced hadron yields is required [277]. Results shown in

[†] We chose $W_{\rm s}$ in lieu of the usual symbol $\lambda_{\rm s}$, which clashes with the strangeness fugacity.

https://doi.org/10.1017/9781009290753.025 Published online by Cambridge University Press

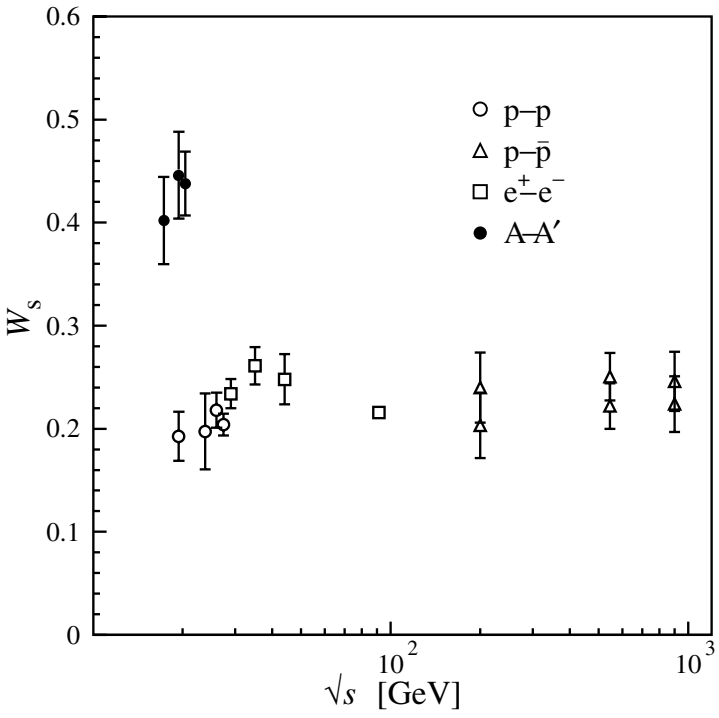

Fig. 18.1. W_s as a function of the center-of-mass energy $\sqrt{s}$ [GeV] (for heavy ion collisions the nucleon–nucleon center of mass energy $\sqrt{s_{NN}}$) [61].

Fig. 18.1 were obtained using a semi-theoretical method [61], in which numerous particle yields are described within the framework of a statistical model, and the computed hadron yields are analyzed in terms of the Wróblewski procedure [277].

We see in Fig. 18.1 that, in elementary p–p, p–$\bar{p}$, and e^+–e^- collisions, the value $W_s \simeq 0.22$ is obtained. In order to estimate the possible influence of the annihilation process on p–$\bar{p}$ reactions, two values of W_s are shown per energy, calculated with initial valence quarks and antiquarks (lower points) and without (upper points). For e^+–e^- interactions, the leading s quarks in $e^+e^- \to s\bar{s}$ have been subtracted [61]. Strangeness is thus relatively strongly suppressed. On the other hand, we also see that, in nuclear A–A′ collisions, W_s more than doubles compared with that in p–p interactions considered at the same energy.

To explain the two-fold increase in yield of strangeness a kinetic model of particle production requires a shift toward production of strangeness in all particle-formation processes. In other words, for modeling the enhanced yields of strangeness within a variety of approaches, see section 6.1, in each model a new reaction mechanism that favors production of stran-

https://doi.org/10.1017/9781009290753.025 Published online by Cambridge University Press

geness must be introduced. Even at this relatively elementary level of counting abundances of hadrons, new physics is evident. In a model with the deconfined phase this new reaction mechanism is due to the presence of mobile gluons, which, as we have seen, are most effective at making pairs of strange quarks. Moreover, because the conditions created in the QGP become more extreme with increasing collision energy, e.g., the initial temperature exceeding substantially the mass of the strange quark, we expect an increase in W_s.

Several among the cascade models we listed in section 6.1 have been tuned to produce not only enough strangeness, but also the observed antinucleons and $\overline{\Lambda}$. However, once this has been done, these hadronic models predict wrong abundances of the rarely produced particles such as $\overline{\Xi}$ and $\overline{\Omega}$. We are not aware of any kinetic hadron model with or without 'new physics' that is capable of reproducing the pattern of production of rare hadrons, along with the enhancement in production of strangeness and hadron multiplicity. Moreover, if rapidity spectra are modeled, usually the transverse momentum spectra are incorrect, or vice-versa. It seems impossible, in a collision model based on confined hadron interactions, to find sufficiently many hadron–hadron collisions to occupy by hadrons the large phase space (high $p_\perp$, high y) filled by products of nuclear collision. If indeed a non-QGP reaction picture to explain heavy-ion-collision data exists, the current situation suggests that some essential reaction mechanism has been overlooked for 20 years. In short, a lot more effort needs to be expended on hadron models in order to reach satisfactory agreement with the experimental results, even regarding rather simple observables such as hadron multiplicities, transverse-energy production, and yield of strangeness.

Another way within the kinetic approach, and within the realm of quite conventional physics, to acquire an excess of strangeness in heavy-ion collisions compared with elementary reactions is to cook dense hadronic matter for a long time. In hadronic gas, strangeness can be produced in unusual (but not novel) reactions such as $\pi + \pi \rightarrow \mathrm{K} + \overline{\mathrm{K}}$. Even in the presence of an abundant yield of pions, the high-mass threshold, compared with the temperatures we are studying here, suggests that their reaction is 'slow'. Thus, an important piece in the puzzle is to know how long it takes for enhancement of strangeness to be created in a kinetic HG fireball. Otherwise, the fact that the final state in all reaction scenarios looks more or less the same will make the argument that the enhancement in production of strangeness is a signature of new physics difficult.

We therefore will consider, in the following section, the dynamics of production of strangeness in thermal processes in HG [164, 165], and we establish the time scales involved. Since the strange quarks are produced as constituents ('valence quarks') of the usual hadronic states, the direct

https://doi.org/10.1017/9781009290753.025 Published online by Cambridge University Press

mechanisms of production will not populate all hadronic states as the phase-space distribution would demand, and therefore, aside from the production, we will also encounter the (relatively rapid) process of strangeness exchange (redistribution) in hadronic quark-exchange reactions. In general, the observed abundances of strange hadrons, and especially of the rarely produced ones, will be the result of multi-step processes.

18.2 Thermal hadronic strangeness production

In a thermally equilibrated central HG fireball the standard

$$\mathrm{N} + \mathrm{N} \rightarrow \mathrm{N} + \mathrm{Y} + \mathrm{K} \tag{18.2}$$

nucleon-based reactions for production of strangeness are, surprisingly, not very important. The hyperon $\mathrm{Y} = \mathrm{qqs}$ may be either the iso-scalar $\Lambda = \mathrm{uds}$ or the iso-triplet $\Sigma = (\mathrm{uus}, \mathrm{uds}, \mathrm{dds})$, and the kaon K may be either $\mathrm{K}^+ = \bar{\mathrm{s}}\mathrm{u}$ or $\mathrm{K}^0 = \bar{\mathrm{s}}\mathrm{d}$, which are found experimentally in one of the (almost) CP eigenstates $\mathrm{K_S}$ and $\mathrm{K_L}$.

There are three reasons for the relative unimportance of the reaction Eq. (18.2):

1. The energy threshold, viz.,

$$\sqrt{s_{\mathrm{th}}} = m_{\mathrm{N}} + m_{\mathrm{Y}} + m_{\mathrm{K}} - 2m_{\mathrm{N}} \sim 670\,\mathrm{MeV}, \tag{18.3}$$

   is considerably higher than, e.g., the energy threshold for production of strangeness in reactions between a pion and a baryon:

$$\pi + \mathrm{N} \rightarrow \mathrm{K} + \mathrm{Y}, \quad \sqrt{\mathrm{s_{th}}} \sim 540\,\mathrm{MeV}\,. \tag{18.4}$$

2. Pions are the most abundant fireball particles, with the pion-to-baryon ratio of the central-rapidity region considerably exceeding unity in all central collisions at above 10 GeV per nucleon. It is for this reason that the reaction

$$\pi + \bar{\pi} \rightarrow \mathrm{K} + \bar{\mathrm{K}}, \quad \sqrt{\mathrm{s}_{\mathrm{th}}^{\pi\pi}} = 710\,\mathrm{MeV}, \tag{18.5}$$

   between two pions, which has also a rather high threshold, is found to be important at temperature $T > 100$ MeV, as we shall discuss.
3. The final-state phase space of the two-particle reaction system above is more favorable than that of the three-body final state required in Eq. (18.2).

The common reaction feature of the hadronic production of strangeness is the $\mathrm{q\bar{q}} \rightarrow \mathrm{s\bar{s}}$ reaction, illustrated for the case of Eq. (18.4) in Fig. 18.2. Note that three of the five (light) quarks are spectators, a $\mathrm{q\bar{q}}$ pair is annihilated, and an $\mathrm{s\bar{s}}$ pair is formed. The experimental value of this

https://doi.org/10.1017/9781009290753.025 Published online by Cambridge University Press

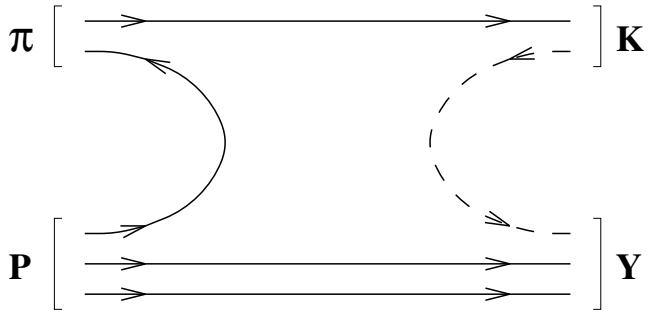

Fig. 18.2. The production of strangeness in reactions of the type $\pi + \mathrm{N} \rightarrow \mathrm{K} + \mathrm{Y}$ in the HG phase. Solid lines indicate the flow of light quarks and the disappearance of one $\bar{\mathrm{q}}\mathrm{q}$ pair, the dashed line is for the added $\bar{\mathrm{s}}\mathrm{s}$ pair.

so-called Okubo–Zweig–Izuka-rule forbidden cross section is about 0.1–0.5 mb in the energy region of interest here (just above the threshold), thus of a magnitude comparable to the cross section for the QGP processes – but the threshold is considerably lower in the QGP processes, and most of the thermal collisions occur in this lower-energy region, as we have shown in Fig. 17.6.

Apart from production of strangeness, we also have 'strangeness-exchange' reactions, as depicted in Fig. 18.3: we see that, in the process, the already existent strange quark can be moved from one particle 'carrier' to another, but the number of strange quarks remains unchanged. We show, in Fig. 18.3, the most relevant class of exchange reactions:

$$\bar{\mathrm{K}} + \mathrm{N} \rightarrow \pi + \mathrm{Y}. \tag{18.6}$$

In an exchange reaction, new hadrons that are difficult to make in direct reactions can be produced. For example, the reaction

$$\Lambda + \bar{\mathrm{K}} \rightarrow \pi + \Xi \tag{18.7}$$

produces the doubly strange particles $\Xi(\mathrm{ssq})$. More generally, exchange reactions distribute strangeness into all accessible particle 'carriers', and help establish the relative chemical equilibrium.

For every strangeness-reaction, there is the same type back-reaction, and one of the two has to be exothermic. Thus 50% of strangeness-exchange reactions are exothermic. Exothermic cross sections do not vanish at small collision energies, and the thermal average is actually nearly a constant $\mathcal{O}(1\ \mathrm{mb})$, which is related to the geometric size and structure of hadrons. Consequently, thermally averaged reaction rates for exchange of strangeness are, especially at low temperatures, much greater than rates of production of strangeness. This assures that strange quarks

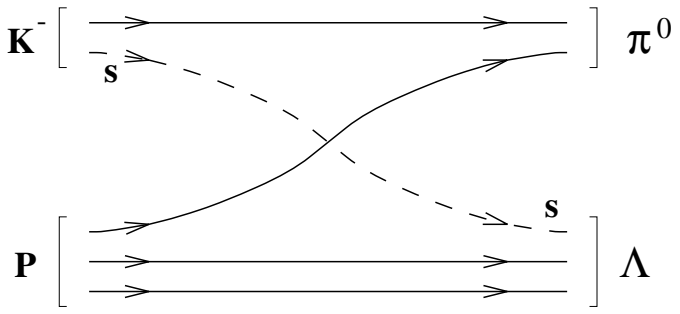

Fig. 18.3. An example of a strangeness-exchange reaction in the HG phase: $K^- + p \to \Lambda + \pi^0$. Solid lines, flow of u and d quarks; dashed line, exchange of an s quark between two hadrons.

produced in HG are rapidly distributed among many hadronic states, even if the absolute chemical equilibrium is not reached.

On the other hand, the cross section for production of strangeness in HG is relatively (to QGP) slow, being suppressed by smaller particle densities and the higher threshold of the production process. Some authors, pursuing explanation of the enhancement in production of strangeness within a HG scenario, try to overcome this in terms of partial restoration of chiral symmetry, which allows hadron masses to melt in part, lowering thresholds for production of strangeness; see [241] for the current status of the search for this effect. We will not pursue further in this book these interesting developments.

In the study of the evolution with time of the production of strange hadrons in the HG fireball, similarly to the case of QGP, only the total numbers of particles will be considered. We are assuming that the thermalization (kinetic equilibration) is a rapid process, in comparison with the relaxation time constant for strange hadrons, and also in comparison with the lifetime of the fireball. To quantitatively develop the kinetic evolution abundances of strange hadrons in the HG, we need to use a large number of hadronic cross sections.

Only limited experimental information on cross sections is available, since it is often impossible to study in the laboratory some of the processes which involve relatively short-lived particles (which of course are quite infinitely long-lived on the scale of hadronic collisions). There is no reliable theoretical framework allowing one to evaluate cross sections not accessible to direct measurement, since our understanding of the hadronic structure is incomplete. Consequently, we consider a method facilitating use of the accessible experimental information, in order to be able to estimate required reaction cross sections.

The cross section times the flux factor (velocity) for two-body reactions $1+2 \to n$, in which n particles are produced in the exit channel, takes the form Eq. (17.9). The generalization of the thermally averaged production cross section Eq. (17.16) to n final-state particles, can be cast into the form

$$R_n = \rho_1\rho_2\langle\sigma_{12}v_{12}\rangle = \frac{g_1g_2}{(2\pi)^5}T\frac{|\mathcal{M}(1+2\to n)|^2}{(2\pi)^{3n-3}} \times \int_{s_{\rm th}}^{\infty} ds\,\sqrt{s}\,{\rm IMS}(s;2){\rm IMS}(s;n)K_1(\sqrt{s}/T), \quad (18.8)$$

where the n-particle invariant phase space is a generalization of the two particle invariant phase space Eq. (17.14):

$${\rm IMS}(s;n) = \int\prod_{i=1}^{n} d^4p_i\,\delta_0(p_i^2-m_i^2)\delta^4\left(p_1+p_2-\sum_i^n p_i\right). \quad (18.9)$$

IMS is implicitly a function of the masses of the particles.

Many studies have shown that the hadronic-reaction matrix element $|\mathcal{M}(1+2\to n)|^2$ for hadronic processes is insensitive to the relatively slow changes of $\sqrt{s}$ in the region of interest to us, and it can be assumed to be constant. For this reason, it is outside of the integral over s in Eq. (18.8). This is the crucial detail which permits us to relate many thermal cross sections to each other: Eq. (18.8) allows us to infer, from an example known experimentally, the thermal average of a family of cross sections. All we need do is adjust the applicable threshold and particle masses. Given the high range of temperatures we are considering, the isospin-breaking effects are relatively unimportant, and one does not distinguish between the u and d quarks. Consequently, one can study isospin-averaged cross sections. Appendix B of [164] gives a useful listing of relevant reactions.

We show now how the method works: the isospin-averaged, thermally averaged associate rate of production of strangeness, $\langle\sigma(\pi{\rm N}\to{\rm K})v_{\pi{\rm N}}\rangle$, can be determined from experimentally known cross sections. It allows us to infer the strength of other associate production processes,

$$\langle\sigma(\pi{\rm Y}\to{\rm K}\Xi)v_{\pi{\rm Y}}\rangle = \langle\sigma(\pi{\rm N}\to{\rm KY})v_{\pi{\rm N}}\rangle P_1, \quad (18.10a)$$

$$P_1 = \frac{\langle\sigma(\pi{\rm Y}\to{\rm K}\Xi)v_{\pi{\rm Y}}\rangle}{\langle\sigma(\pi{\rm N}\to{\rm KY})v_{\pi{\rm N}}\rangle}, \quad (18.10b)$$

where P_1 in Eq. (18.10b), with the assumption of constant $|\mathcal{M}|^2$, depends on T and $\mu_{\rm b}$ only through its dependence on the particle phase space.

The thermal averages of cross sections falling under the categories 'strangeness exchange' and 'baryon annihilation' can also be dealt with

https://doi.org/10.1017/9781009290753.025 Published online by Cambridge University Press

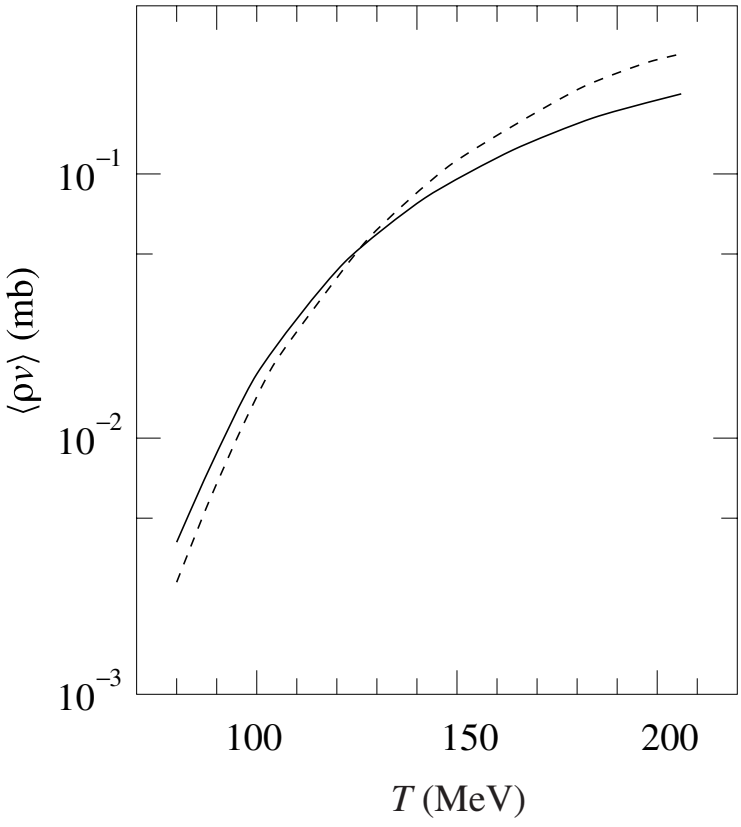

Fig. 18.4. The thermally averaged $\pi\pi \to K\bar{K}$ reaction cross section: the solid line is for a constant matrix element (see the text); the dashed line is for a constant value of the reaction cross section, $\sigma = 3$ mb [164].

in this way. The various strangeness-exchange cross sections are related to $\langle \sigma(\bar{K}N \to Y\pi) v_{\bar{K}N} \rangle$ and diverse baryon-annihilation cross sections to $\langle \sigma(p\bar{p} \to 5\pi) v_{p\bar{p}} \rangle$, which are known experimentally. Similarly, the matrix element $|\mathcal{M}|^2$ for reactions in which particles and antiparticles are interchanged is the same, and the average thermal cross sections of the reverse reactions are given by those of the forward reactions times appropriate phase-space factors.

This method leaves us with one important channel, Eq. (18.5), for production of strangeness in the thermally equilibrated hadronic gas, which can neither be measured nor be related to known reactions. Its strength has been derived from the reactions $pp \to pp\pi\pi$, $ppK\bar{K}$ with the help of dispersion relations. Protopopescu *et al.* [210] have found that, above the threshold, pion-based production of strangeness has an approximately constant cross section of 3 ± 1 mb. The thermally averaged cross section

https://doi.org/10.1017/9781009290753.025 Published online by Cambridge University Press

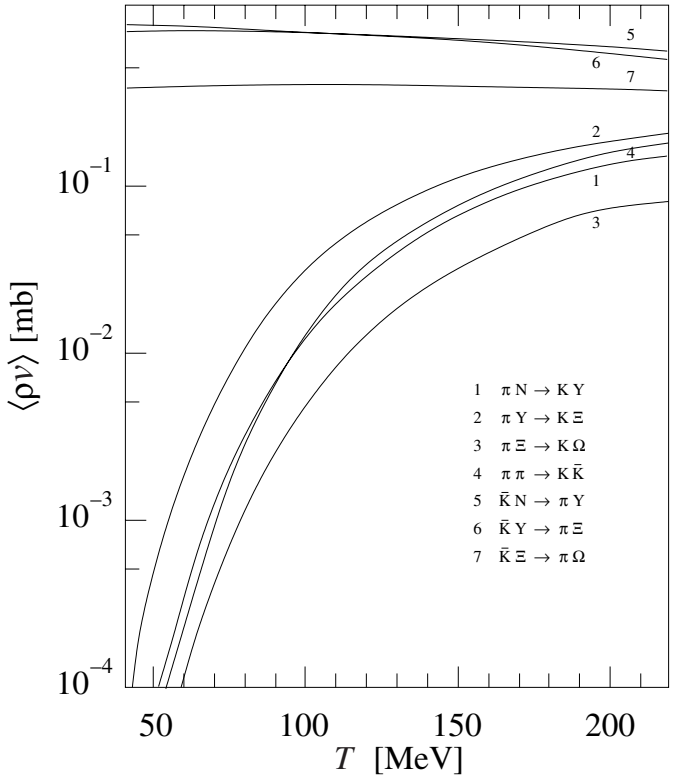

Fig. 18.5. Thermally averaged cross sections for formation and exchange of strangeness in HG $\langle \sigma v \rangle / c$, based on the assumption of universal invariant matrix elements [164].

using as input a constant cross section of 3 mb is shown in Fig. 18.4 by the dashed line, as a function of temperature. In comparison, the solid line describes the result of an evaluation in which a constant matrix element $|\mathcal{M}|^2$ was used with the strength equal to the associate reaction for production of strangeness $\pi + \mathrm{N} \to \mathrm{K} + \mathrm{Y}$.

In Fig. 18.5, we show the thermally averaged cross sections for formation and exchange of strangeness obtained by Koch *et al.* [164] within the framework outlined above. Note that the thermally averaged strangeness-exchange reactions which are capable of building up multiply strange hadrons are $\mathcal{O}(1\ \mathrm{mb})$ at all temperatures. This is consistent with the intuition that this value should be at the level of a third of the geometric cross section, multiplied by the probability of exchanging one of the quarks, which is at the level of 10%, certainly not 100%, as is sometimes assumed by some authors. Even though (by coincidence) reactions 5 and 6 agree in strength, reaction 7, which is important for understanding the formation

https://doi.org/10.1017/9781009290753.025 Published online by Cambridge University Press

of Ω, is considerably smaller. This strongly breaks the $SU(3)$ flavor symmetry, and slows down the formation of the all-strange Ω and $\overline{\Omega}$ in HG, compared with the formation of other strange baryons and antibaryons.

We further see in Fig. 18.5 that strangeness-formation reactions in HG are dominated at high temperature by the $\pi\pi \to \mathrm{K}\bar{\mathrm{K}}$ reaction. Up to temperatures near $T = 150\,\mathrm{MeV}$, strangeness-exchange reactions 5 and 6 are more than an order of magnitude faster than is the production of strangeness. Thus, relative chemical equilibrium can be established 'instantaneously' in singly and doubly strange hadrons, but not for Ω and $\overline{\Omega}$, during the growth in abundance of strangeness in the fireball. For the same reason, it makes good sense to expect relative chemical equilibrium among strange hadrons to occur in an equilibrium model of hadronization of QGP, except for Ω and $\overline{\Omega}$.

18.3 The evolution of strangeness in hadronic phase

To address the issue of equilibration of strangeness in HG in a quantitative manner, we study the temporal evolution in the framework of a master equation. We consider all two-body reactions, which are predominant,

$$\frac{d\rho_i(t)}{dt} = \sum_{\mathrm{AB}} \langle \sigma v_{\mathrm{AB}\to i} \rangle_T \rho_{\mathrm{A}} \rho_{\mathrm{B}} - \sum_{\mathrm{C}} \langle \sigma v_{i\mathrm{C}\to \mathrm{X}} \rangle_T \rho_i(t) \rho_{\mathrm{C}}, \tag{18.11}$$

where the collision of particles A + B leads to production of the strange particle i, and i can be annihilated in collisions with (strange) particles C. Assuming the thermal momentum distribution of all particles Eq. (17.16) permits one to compute the evolution of particle populations using Eq. (18.11), once the thermal cross sections of the reaction are known; see section 18.2. Appendix A of [164] gives the explicit form of the master equation Eq. (18.11).

In HG antibaryons are difficult to produce, considering that the direct pair-production thermal cross section for $\pi + \pi \to \mathrm{N} + \bar{\mathrm{N}}$ is suppressed by a high threshold. Intermediate steps are necessary in order to build up heavy mesons, e.g., ρ and ω resonances, which are more capable of producing a baryon–antibaryon pair, and which also benefit from a larger elementary cross section. A recent kinetic-theory study of reactions involving fusion of three mesons into antibaryons suggests that this channel may be the dominant source of antibaryons [89].

In order to establish an upper limit for the abundance of multistrange baryons in HG, the results shown below were obtained assuming that the non-strange antibaryons are at the chemical HG equilibrium yield at the initial time, at which the evolution of the master equation is considered. In this approach, the build-up of strange antibaryons is a function of the developing abundance of strangeness, and the effectiveness

https://doi.org/10.1017/9781009290753.025 Published online by Cambridge University Press

of strangeness-exchange reactions, which as we have seen is particularly weak for the formation of the most enhanced $\overline{\Omega}$. Even allowing full occupancy of non-strange-antibaryon phase space, the relaxation time for yields of strange antibaryons in HG turns out to be much too long to be relevant in a dynamic heavy-ion-collision environment. In fact, the discovery of abundant yields of strange antimatter that sometimes exceed chemical equilibrium in heavy-ion collisions is proof that collective formation mechanisms akin to those operating in quark-soup hadronization have been operational.

Somewhat surprised by the high yield of (strange) antibaryons observed in heavy-ion collisions, some authors have proposed to use detailed balance considerations to infer an effective rate of five-hadron collisional production of a baryon–antibaryon pair, using as reference in detailed-balance analysis the reverse reaction $\mathrm{N} + \bar{\mathrm{N}} \rightarrow 5\pi$. In our opinion, use of detailed-balance arguments to infer a five-body collisional reaction rate is wrong physics. Certainly five-particle collisions occur more rarely than do four-particle collisions, which occur more rarely than do three-particle collisions, etc. One has first to establish the dominant forward *and* backward channels (if such exist, for equilibrium could be the result of multistep processes) when one is using the detailed-balance argument to estimate a rate. For the case of baryon–antibaryon formation and annihilation in HG, depending on temperature and density, two- and three-body reactions among mesons should dominate higher many-body processes.

We shall now review a few properties of the solutions of the master equations Eq. (18.11). To maximize the yield of strangeness that can be obtained, and to maximize the production of strange antibaryons, we assume that, after $\tau_0 \simeq 1$ fm, the densities both of pions and of antinucleons should have reached approximately their chemical-equilibrium values, and, at this point in time, the thermal processes for production of strangeness are turned on in HG. First, we turn our attention to the evolution of the total yield of strangeness in the HG phase assuming that the initial densities of strange particles are zero. Then, we consider the evolution of the yields of individual strange hadrons, including strange antibaryons.

We study the total strangeness in HG, to determine the time required for the total abundance of strangeness to reach the chemical equilibrium. In Fig. 18.6, the evolution of the total abundance of strangeness is shown, and we see that the production of strangeness in HG is roughly 100 times slower than the time for chemical relaxation in QGP, see Fig. 17.11, for the example of temperature $T = 160\,\mathrm{MeV}$. The considered range of the baryo-chemical potential $\mu_\mathrm{b} \in [0, 450]\,\mathrm{MeV}$ covers all regions of interest and, as we see, has a negligible impact on this result.

https://doi.org/10.1017/9781009290753.025 Published online by Cambridge University Press

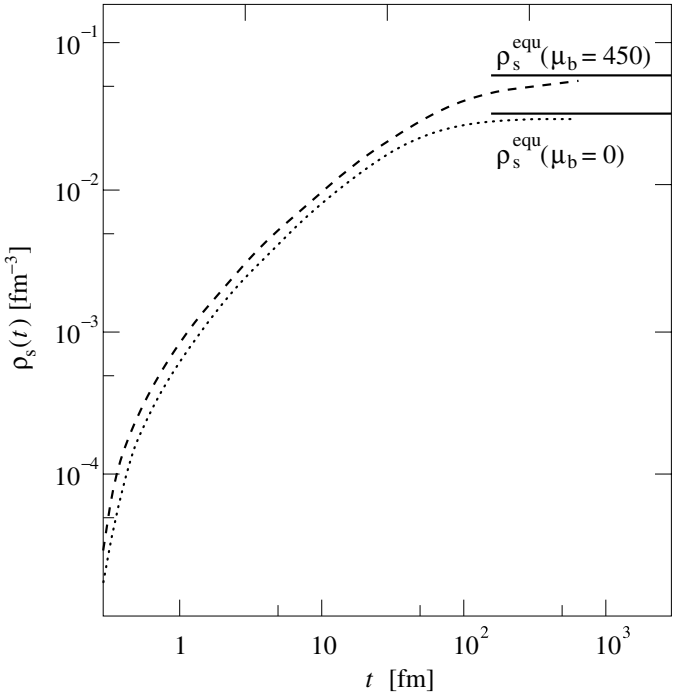

Fig. 18.6. The thermal production of strangeness as a function of time in a confined hadron gas at $T = 160\,\mathrm{MeV}$. Results for two values of baryo-chemical potential ($\mu_\mathrm{b} = 0$ and $450\,\mathrm{MeV}$) are shown [164].

The yield of strangeness observed in experiments at the SPS and RHIC can not be produced by thermal HG processes. This becomes even clearer on considering individual particles with higher strangeness content such as (multi)strange antibaryons, shown in Fig. 18.7. For reasons we discussed above, strange antibaryons remain more distant from the equilibrium distribution than do strange mesons and strange baryons. In fact, to arrive within the time scale shown at a measurable yield, the result presented benefits from the rather optimistic assumptions of equilibrium abundances for the non-strange antibaryons. As expected, we see in Fig. 18.7 that kaons, $\mathrm{K} = \bar{\mathrm{s}}\mathrm{q}$, antikaons, $\bar{\mathrm{K}} = \mathrm{s}\bar{\mathrm{q}}$, and hyperons, $\mathrm{Y} = \mathrm{qqs}$, are the first to reach equilibrium abundance – the other $\bar{\mathrm{s}}$ carriers are delayed by another factor of 3–5 in getting to their HG limits, with $\overline{\Omega} = \bar{\mathrm{s}}\bar{\mathrm{s}}\bar{\mathrm{s}}$ trailing far behind. We expect that the HG-based production of multistrange antibaryons generates negligible background. This is one of the important reasons allowing multistrange antibaryons to signal the formation and hadronization of a deconfined quark–gluon phase in heavy-ion collisions.

https://doi.org/10.1017/9781009290753.025 Published online by Cambridge University Press

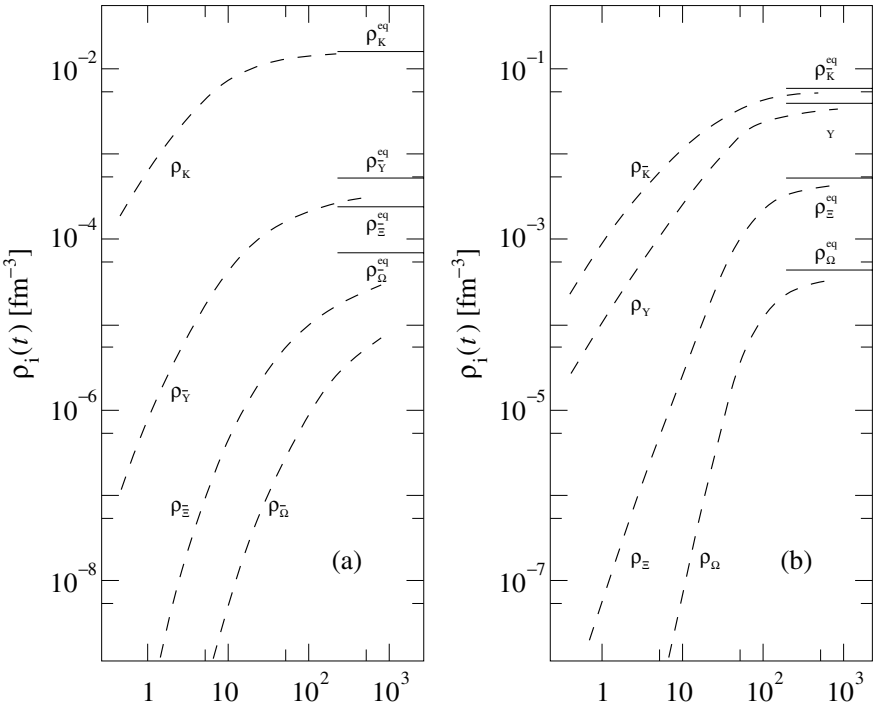

Fig. 18.7. The approach to chemical equilibrium by strange hadrons in hot hadronic matter at temperature $T = 160$, $\mu_b = 450\,\mathrm{MeV}$ – $\bar{s}$ hadrons are shown in (a), whereas s hadrons are shown in (b) [164].

19 Hadron-freeze-out analysis

19.1 Chemical nonequilibrium in hadronization

In the final state, we invariably see many hadronic particles, and naturally we observe their spectra and yields only in restricted domains of phase space. An extra reaction step of 'hadronization' is required in order to connect the properties of the fireball of deconfined quark–gluon matter, and the experimental apparatus. In this process, the quark and gluon content of the fireball is transferred into ultimately free-flowing hadronic particles. In hadronization, gluons fragment into quarks, and quarks coalesce into hadrons.

Hadronization of course occurs in all reactions in which final-state hadrons are observed: for example, in high-energy $e^+e^- \to q\bar{q}$ reactions, we see jets of final-state hadrons carrying the energy and momentum of the two quarks produced. It is not yet clear whether there is a fundamental difference between the hadronization of a thermal fireball and that of a

https://doi.org/10.1017/9781009290753.025 Published online by Cambridge University Press